How rapidly do the southern subtropical oceans respond to wind stress changes?

Darryn W. Waugh[1,2*], and Thomas W. N. Haine[1]

[1]*Department of Earth and Planetary Sciences, Johns Hopkins University, Baltimore, MD*

[2] *School of Mathematics and Statistics, University of New South Wales, Sydney, New South Wales, Australia*

Corresponding author: Darryn Waugh (waugh@jhu.edu)

Key Points:

- There is a decadal to century response time for ideal age, temperature, and salinity in mode waters to an increase in the wind stress.
- The response time of the ideal age to an increase in wind stress is much younger than the ideal age itself.
- Wind-driven trends in ideal age, temperature, and salinity may continue for several decades even if there is a pause in wind stress trends.

Abstract

The response time of the southern subtropical oceans to an increase in the wind stress is examined in a climate model perturbation simulation where there is an abrupt increase in the wind stress. The ocean response time is shown to vary among fields: The intensification of the gyres and vertical movement of isopycnals happens over 5-10 years, while the change in ideal age, temperature, and salinity in mode and intermediate waters occurs much slower, with the response time exceeding 100 years at depths of 500-1000 m. While the response time for ideal age is longer than that for the surface circulation it is notable that it is much younger than the ideal age itself. The different response times indicate that changes in the winds over the southern oceans and in the horizontal circulation / density structure will occur near simultaneously, but there may be a substantial lag in subsurface changes from wind changes and these may persist for decades even if no further changes in the winds occurs.

Plain Language Summary

The time it takes properties of the southern hemisphere subtropical oceans to respond to changes in the westerly winds blowing over the oceans is examined using a simulation of the climate model in which the wind stress is abrupted increased. This idealized simulation enables the response time to be easily quantified, and it is shown that there is a wide range of response times among ocean properties. The increase in the horizontal circulation and vertical movement of surfaces of constant density happens over around 5 years, whereas the response time of temperature, salinity, and mean transit time within the ocean interior can exceed 100 years. This means that while changes in the horizontal circulation will occur near simultaneously with changes in the winds, there will be a substantial lag in changes in subsurface properties and these properties will be insensitive to year-to-year variations in the winds.

1 Introduction

Changes in a wide range of characteristics of the southern oceans have been observed over the last few decades, including changes in the heat and carbon content (e.g., Cai et al. 2010, Le Quéré et al., 2007), the Antarctic circumpolar current (e.g., Boning et al 2008), strength of the subtropical gyres (e.g., Roemmich et al. 2007, 2016), ventilation ages (e.g., Waugh et al. 2013, Ting and Holzer 2017), and mode water properties (Gao et al. 2018). Many of these changes have been linked to the intensification and poleward shift of the surface westerly winds over the same period (e.g., Thompson et al. 2011, Swart and Fyfe 2012). However, while the above ocean changes are qualitatively consistent with the expected response, it is difficult to attribute the ocean changes to the wind stress changes because of a lack of a quantitative understanding of the response of ocean properties to changes in wind stress.

One aspect where improved understanding is required is the transient nature of the ocean response. While it is expected that different aspects of the oceans will respond to wind stress perturbations over different time scales (e.g., there will be a slower response for tracers within the ocean interior than the response of ocean surface circulation, just as it takes longer for simulations of ocean tracers to reach equilibrium than for the surface circulation), how the transient response differs between fields and spatially has not been quantified. This quantification is important for both interpreting observed ocean changes and making projections of future changes. For example, whether observed ocean changes should be linked with simultaneous changes in wind stress or to the lagged or time-integrated change in wind stress depends on the response time of the ocean property. This response time also determines how long changes in the ocean persist after a change in the wind forcing depends on the response time of the particular ocean property.

This latter issue is particularly important given past and projected changes in the wind stress over southern mid-latitudes. Meteorological reanalyses show an increase and poleward shift in the summer-time wind stress over southern mid-latitudes between 1970 and 2000, but there has been little change in strength and latitude of peak summer winds since 2000 (Banerjee et al. 2020). This ‘pause’ in trends is consistent with climate model simulations which show an increase/poleward shift from 1975 to 2000 (due primarily to the formation of the ozone hole) and then no trend from 2000 to ~2030 (as ozone hole stabilizes and any recovery is balanced by continued growth of CO_2) (Barnes et al. 2014). It is unknown how quickly the oceans will respond to this pause in wind stress trends, i.e., will the trends in ocean properties discussed above also pause, or will there be a time lag and persistence of ocean trends even when no trends in the wind stress?

Here we address the above questions by examining the transient response of the subtropical oceans in a climate model simulation in which there is an abrupt increase in the wind stress over the southern oceans. Numerous studies have examined the long-term response of the ocean circulation, hydrography, and tracer distributions to an abrupt change in wind stress (e.g., Sijp and England 2008, Farneti et al. 2010, Gent and Danabasoglu 2011, Spence et al. 2014, Waugh 2014, Downes et al. 2017, Hogg et al. 2017, Waugh et al. 2019), but little attention has been paid to time scales for these responses. Here we quantify, for the first time, the transient response of multiple aspects of the southern subtropical oceans to an increase in wind stresses. Specifically, we examine the response of the barotropic transport stream function, density, ideal age, temperature, and salinity fields. We consider the ideal age as it equals the mean time for transport from the surface to an interior location, a fundamental property of the ocean transport.

Also, recent studies have shown changes in the age of southern mode waters inferred from observations (e.g., Waugh et al 2013, Tanhua et al. 2013, Ting and Holzer 2015, Fine et al. 2017), and suggested that this is due to changes in the wind stresses. However, quantification of the transient response of the age is required to test this suggestion. Finally, changes in age can provide information on (be used to estimate) changes in oceanic anthropogenic carbon, heat, and oxygen (e.g. Russell et al. 2016).

The model experiments and analysis methods are described in the next Section. In Section 3 we briefly discuss the long term (100 year) response of the fields, and then in Section 4 examine the evolution and responses times. In Section 5 linear response theory is used to estimate the response of the fields for arbitrary time-varying changes in the wind stress. Concluding remarks are in the final section.

2. Model Experiments

We examine the output from a wind-stress perturbation simulation performed in the Community Climate System Model version 4 (CCSM4) (Gent and Danabasoglu 2011). CCSM4 is a fully coupled atmosphere-ocean model as documented in Gent et al. (2011). The ocean component has 60 vertical levels, with horizontal resolution around 1^o. Mesoscale eddies are not resolved and are parameterized using a Gent and McWilliams eddy parameterization with a coefficient k that is a function of space and time.

In the wind-stress perturbation examined here the wind stress forcing is multiplied by the factor 1.5 south of 35^oS from that in a long preindustrial control run (which will be referred to simply as the "control" run). This results in increases of the maximum zonally averaged zonal wind stress from 0.19 to 0.28 N m^{-2} but does not change the latitude of the maximum wind stress (**Figure 1a**). This perturbation is not meant to represent the past changes in southern winds, which involve changes in location as well as strength of peak winds as well as zonal variations in the wind changes, but rather to provide a clean experiment to isolate the response to an increase in wind stress.

The wind-stress perturbation simulation is run for 100 years, and the control simulation is also extended for 100 years. There is interannual variability in the wind stresses in both the control and perturbation simulations, but the magnitude of this variability is much less than the difference in wind stress between simulations (e.g., the interannual standard deviation of the maximum wind stress in the control simulation is 0.01 N m^{-2} is much smaller than the mean difference of 0.09 N m^{-2} between simulations).

As described in Gent and Danabasoglu (2011), the increased zonal wind stress in the perturbation simulation does not directly affect the atmosphere-to-ocean heat and freshwater fluxes. But there is an indirect effect on the coupled system through changes to the sea surface temperature caused by the stress change, which results in changes in air-sea fluxes between simulations. The differences in these fluxes between simulations are small, however: the large-scale patterns of the fluxes are the same, and the differences that occur are generally associated with small shifts in localized regions of high fluxes.

We consider the response of several different fields: The barotropic stream function (BSF), potential density referenced to 2000 dbar (σ_2), temperature (T), salinity (S), ideal age (Γ). The ideal age is a tracer that yields, in the limit of long times compared to the circulation, the mean time since water last made surface contact (e.g., England 1995, Hall and Haine 2002).

The response of a given field is calculated as the difference between the perturbation and control simulations evaluated at the same time. To quantify the time scale of the response we fit the time series of the specified field with the function

$$R(t) = R_0(1 - e^{-t/\tau}) \quad (1)$$

where R_0 is the steady-state response and τ the e-folding time of the response (which we refer to as the response time). The steady-state response R_0 of some of the fields considered has been examined in previous studies (Gent and Danabasoglu 2011, Waugh 2014), but the response time τ has not. The response time τ should not be confused with the ideal age, and, as will be shown below, τ is generally not the same as the ideal age Γ.

3. Long-term Response

Before examining the temporal variation in fields of interest we briefly examine the response 100 years after the perturbation is applied. The changes in σ_2, Γ, and T after 100 years in these simulations have been examined in more detail in Gent and Danabasoglu (2011) and Waugh (2014). **Figure 1b-h** shows the response (difference between the two simulations) of the BSF, σ_2, Γ, T, and S fields at 100 yr.

There is an increase in the magnitude of the BSF (more negative BSF) throughout most of the subtropical oceans (**Figure 1b**), which corresponds to an intensification of the subtropical gyres. As shown in previous studies (e.g., Saenko et al. 2005, Cai 2006, Cai and Cowen 2007, Waugh et al 2019), this response is consistent with Sverdrup balance, i.e., there is an increase in the wind stress curl north of 50^{o}S and within this region the magnitude of the BSF increases.

The change in wind stress curl also leads, via Ekman pumping, to changes in the density structure (**Figure 1c**). There is a shoaling (upward movement) of isopycnals south of 45^{o}S where the wind stress curl decreases, and deepening (downward movement) of isopycnals north of 45^{o}S, except near the surface. This movement of isopycnals corresponds to a steepening (increase in horizontal gradients) of isopycnals across the Antarctic circumpolar current. Note, although the simulations do not resolve eddies, the eddy parameterization coefficients are a function of space and time, which results in partial eddy compensation (Gent and Danabasoglu 2011, Gent 2016).

As shown in Waugh (2014), there is a significant decrease in ideal age (i.e. age decrease is much larger than the interannual variability and trend of the control run) within mode and intermediate waters (35.5 kg/m^3 < σ_2 < 36.5 kg/m^3)in the CCSM4 wind stress perturbation, see **Figure 1d**. It is notable that the spatial structure and magnitude of the age response is very similar to that for the abrupt increase wind perturbation in the 0.25^o ocean-sea ice model simulation examined in Waugh et al (2019). In both simulations the peak decrease in age exceeds 50 years and occurs around 35^{o}S and 1000-1500 m depth. The agreement suggests that a coarse-resolution climate model with parameterized eddies (e.g., CCSM simulation considered here) may produce a similar change in ideal age as a higher resolution eddy permitting model.

The change in age is due to both transport along isopycnals and movement of isopycnal surfaces. We decompose the change in age at fixed depth (the "total" change) into the change due to transport along isopycnals ("isopycnal" change") and that due to the wind-driven movement of isopycnals ("heave"; Bindoff and McDougall (1994)). The isopycnal change is

determined by calculating the change in age at fixed density (for each latitude) and then mapping this to depth space using the the control density distribution. The change due to heave is calculated by mapping the perturbation age in density space into depth space using the control density distribution, and then taking the difference from the control age in depth space.

Figures 1e,f show the heave and isopycnal change in age. The spatial structure of the age change differs between processes: Heave produces an increase in age between 45 and 60 ^{o}S but a decrease between 20 and 40 ^{o}S (consistent with changes in density shown in **Figure 1c**), whereas isopycnal change produces a decrease throughout mode and intermediate waters. The largest changes in age at fixed depth (**Figures 1d**) occur in regions where heave and isopycnal change cause the same sign change in age (e.g. both cause a decrease in age around 1000m, 35^{o}S), while the smallest change occurs in regions where they oppose each other (e.g. 200-1000m, 50^{o}S). The relative role of changes in age due to heaving and isopycnal transport shown in **Figure 1** is again consistent with the eddy-permitting simulations analyzed in Waugh et al (2019).

The increase in the wind stress also results in changes in the temperature and salinity fields. As shown in **Figures 1g,h** there is an increase in both zonal-mean T and S through most of mode and intermediate waters. The spatial structure of the response is somewhat different between the two fields: The maximum total change in T occurs around 1000 m between 30 and 40^{o}S, whereas maximum increase in S occurs further south and at the surface (above 500 m and around 55^{o}S). This difference in spatial structure is because the impact of heave varies between fields. As there are only weak vertical S gradients (contours in **Figure 1h**) the movement of isopycnals (heave) has only a small impact on S. In contrast there are strong vertical gradients of T through mode and intermediate water, and like age, there are substantial changes in T due to heave. The pattern of the isopycnal changes in T and S are the same (as they must be), with both fields increasing in mode and intermediate waters with the maximum increase nearer the surface around 55^{o}S (see contours in **Figures 3d** below).

4. Response Time

We now examine the evolution of the above fields, and how long it takes the fields to reach a new statistically-steady state following the abrupt wind change. We first consider the response of the BSF. **Figure 2a** shows that the intensification of the gyres (decrease in minimum BSF) happens rapidly, with the vast majority of the decrease in the minimum BSF in each basin occurring within the first 10 years. Fitting the minimum BSF time series with equation (1) yields response times τ~3-6 years. Similar short response time scales are also found for individual locations within the subtropical gyres (not shown). This ~5 year spin-up time is similar to that in previous studies examining the response of subtropical gyres to changes in wind stresses (e.g., Deser et al.1999, Thomas et al. 2014), which linked the response time to the basin crossing time of baroclinic Rossby waves. Note that in the presence of topography there is an interaction between baroclinic and barotropic modes which results in a slow adjustment of the barotropic mode on the time scale of the baroclinic modes (e.g., Anderson and Killworth 1977, Anderson et al. 1979).

There is also generally a fast response in the density structure, with the upward or downward movement of isopycnals occurring primarily in the first 20 years. This is illustrated in **Figure 2b** for three locations with initial σ_2=36.0 kg/m^3 (see diamonds in **Figure 1**). At the

southern-most location shown (49°S) there is an increase in σ_2 over the first 20 years (τ~10yrs), while at the northern-most location (36°S) there is a rapid decrease (τ~5yrs). At 43°S there is only a weak change in σ_2 (consistent with **Figure 1c**) and τ~90yrs. For latitudes between 30°S and 55°S the response time is 5-10 yrs except in the regions where where there is little change in density, see **Figure 3a**. Note, in **Figure 3a** values are not shown if equation (1) is a poor fit to the response (i.e., if the root-square mean difference divided by the mean change exceeds two). North of 30°S, where there is no change in the wind stress (**Figure 1a**), the decrease in σ_2 at fixed depth occurs more slowly, with a roughly linear increase over the 100 years of the perturbation simulation (not shown). This slow deepening of isopycnals is consistent with theory and idealized modeling showing a centennial timescale for deepening of the global pycnocline due to interactions between the Southern Ocean and northern basins (Jones et al. 2011; Allison et al. 2011).

The response time of Γ varies with latitude and depth, and also between isopycnal and heave change. This is illustrated in **Figure 2c-e** which shows the time series of the change in zonal-mean Γ for the three locations discussed above, for the total, heave, and isopycnal change, respectively. As expected, the evolution (and response time) of the change in age due to heave is very similar to that for the change in density.

There is a large variation in τ for the isopycnal change in age (**Figures 2e, 3d**). Near the surface τ is less than 5 years but τ increases with depth, and exceeds 100 yrs at deep, northern latitudes. The longer response time of the ideal age compared to that of the BSF and density occurs because the BSF and density response times are controlled by wave dynamics (most likely the basin crossing time of Rossby waves) whereas the ideal age response is controlled by the advection and mixing of tracers from the surface to the interior location which occur over longer time scales.

There is generally a monotonic increase in τ with more equatorward locations along an isopycnal, with τ increasing roughly linearly with distance from the outcrop for 10-15° degree north of an outcrop, see **Figure 4a**. The ideal age also increases roughly linearly with distance from the outcrop but more rapidly than τ, see **Figure 4b**. This means that τ is much younger than Γ, see **Figure 4c**. This is somewhat surprising as the ideal age is the mean time for transport from the surface to interior location, and it might be expected that the time to respond to changes in the circulation will be similar to this mean transport time. In addition, for the simple case of uniform advection with no mixing the time for the ideal age (which equals the distance from source divided by advection speed) to come to a new steady state after an abrupt increase in flow speed is equal to the age in the new state, i.e. $\tau = \Gamma$.

Why the response time of the age in mode and intermediate waters in the CCSM perturbation simulation is much less than the age itself is unknown. Possible insights into the difference between t and Γ come from comparison of the slopes of their relationships with latitude. The slope of the latitude- τ relationships are around 0.2-0.3 cm/s (solid lines in **Figures 4a**). This "propagation" speed is of similar order to the time-mean meridional flow in the gyre (away from the western boundary current), possibly suggesting that τ may be determined primarily by the advective timescale. There is a smaller slope of the latitude-Γ (~0.01-0.04 cm/s; solid lines in **Figures 4b**), corresponding to slower "propagation" of Γ. Thus Γ is larger than the advective time, consistent with mixing playing a major role in

determining Γ. This suggests the age response time is determined primarily by the advection of young waters to a given location, whereas the ideal age is influenced also by mixing with older (recirculated) waters. Further analysis is required to determine if this indeed the case, but is beyond the scope of this work.

The transient response of Γ at fixed depth differs between regions with differing balances between heave and isopycnal changes (**Figures 2c, 3c**). Between 30 and 40^{o}S where both heave and changes in along-isopycnal transport cause a decrease in age the response time of Γ at fixed depth is generally less than that due to isopycnal transport, as the deepening of isopycnals (and decrease in age at fixed depth) occurs more rapidly than the decrease due to isopycnal transport. South of 40^{o}S the isopycnals shoal and the age change due to heave opposes that due to along-isopycnal transport, and there is generally only a small change in age at fixed depth after 100 years (Figure 1). The time to reach the 100-yr change increases with depth, but for many locations the equation (1) is a poor fit for the response and τ cannot be defined using this relationship. This occurs because the initial (~5-10 yr) increase in age due to shoaling is of similar magnitude to the long time decrease due to along-isopycnal transport. The response in this region could be fit by a two-time scale equation (i.e. a second exponential term in equation 1) but we have not done this as the change age in this region is very small (Figure 1).

The response times for T and S share similarities with that for Γ: The response times for T and S vary spatially (latitude and depth), between isopycnal and heave change, and are generally much slower than the BSF and density responses. The timescale for heave changes in T and S are generally less than 5 years and similar to that for age (and vertical movement of isopycnals), and are not shown. However, the response time τ for isopycnal changes in T and S is in most regions greater than τ for isopycnal changes in age, see **Figures 2** and **3**. As the evolution of T and S on isopycnal surface is the same, we only show the evolution and response time for T in **Figures 2** and **3**.

While isopycnal changes (decreases) in ideal age occur because of more rapid surface to subsurface transport, this is not the primary cause of the isopycnal increases in T or S. As both T and S increase with depth along isopycnals, more rapid along-isopycnal transport would bring lower tracer values to depth and cause a decrease in subsurface T and S, and not the increases in T and S. Instead, the primary cause is increases in mixed layer T and S where the σ_2 = 35.5-36.5 kg/m^3 isopycnal surfaces outcrop (55-65^{o}S). The increases in near-surface T and S occur within the first 5 years (see **Figure 5**), and are consistent with increases in the northward Ekman flow and upwelling in subpolar regions from increased wind stress (e.g., Ferreira et al. 2015). These T and S anomalies then propagate along isopycnals into subtropical mode/intermediate waters. As the ideal age is set to zero in the surface layer, this process does alter the ideal age in mode/intermediate waters.

Although the propagation of larger mixed layer T and S into the interior is likely the major cause of the isopycnal changes in these tracers, the increase in the rate of transport (decrease in ideal age) may still play a role. For example, there are only small changes in T and S along the isopycnals where the largest decreases in age occur (σ_2=36.5-37.0 kg/m^3), possibly because of cancelation between increased mixed layer values and more rapid along-isopycnal transport into the interior.

5. Linear Response Functions calculations

The wind stress perturbation considered above is idealized, and the response cannot be directly compared with observations. However, assuming a linear response, the temporal evolution of a given field (e.g. BSF, age) from an abrupt wind-stress perturbation can be used together with "linear response function" theory to estimate the temporal evolution of the field for arbitrary time-varying changes in the wind stress.

If R(t) is the linear transient response of a system variable Φ to a step function increase at time t=0 in a specified forcing, then the linear response of the variable Φ to arbitrary forcing F(t) (with F=0 for t<0) is (e.g., Hasselmann et al. 1993)

$$\Phi(t) = \int_0^t R(t-t')\frac{dF}{dt'}(t')dt' \,. \qquad 2)$$

Thus once R is known the change in variable Φ for any time variation in the forcing can be determined from (2). This approach has been used to examine the response of atmospheric surface temperatures to increases in CO_2 (e.g., Hasselmann et al. 1993) and more recently the sea surface temperature response to increases in CO_2 or ozone depletion (e.g. Marshall et al. 2014).

Here we will apply (2) to the wind-stress perturbation experiment, and examine the response of ocean fields to different temporal variations in the magnitude of the wind stress. In this case the wind-stress corresponds to the forcing F, and the time series of ocean field (BSF, Γ, T, S, etc) in the abrupt perturbation simulations is, when appropriately scaled, equal to the response function R. Equation (2) is then used to estimate the change in ocean field for arbitrary temporal variations in the wind stress perturbation. A potential issue with this calculation is the assumption of linearity. However, analysis of simulations with an increase, a shift, and combined increase and shift of winds in Waugh et al (2019) suggest the response of the age in mode and intermediate waters is close to linear.

As discussed in the Introduction, observations and models indicate an intensification and poleward shift of the summer wind stress over the last few decades of the 20th century, but a pause, or even slight reversal, in these trends since around 2000 (Banerjee et al. 2020, Barnes et al. 2014). Given this we consider the idealized case where there is a linear increase in the magnitude of the wind stress from 1970 to 1999, followed by 30 years (2000-2029) with no change in the wind stress (thin lines in **Figure 6a)**. This could be considered an idealization of the response to the formation of the Antarctic ozone hole and then stabilization. To see the impact of year-to-year variations we include a small oscillatory perturbation with period of 5 years to the these trends (thick curve in **Figure 6a)**.

The simulated response of specific fields in CCSM4, such as shown in **Figure 2**, can be used to estimate the response functions R(t) in the convolution (2). Rather than using the simulated response we consider for simplicity R(t) of the idealized form of equation (1), with τ varying between 5 and 100 yrs (**Figure 6b**). This R(t) can be used to estimate the response of different fields (at different locations). For example, τ = 5 yrs is representative of change in the BSF, density, and near surface age, T and S, while τ = 50 and 100 yrs are representative of change in age, T and S at mid-depths.

Figure 6c shows the response to the wind stress changes shown in **Figure 6a** for the different response functions in **Figure 6b**. There is a decrease with time for all τ, but (i) the amplitude of the 5-year variations and (ii) the longer term rate of decrease varies dramatically with τ. Only for τ = 5 yrs are there noticeable oscillations about longer term decrease and even then the amplitude is much less than for the wind stress. In other words, for response times around and larger than τ = 10 yrs the response is insensitive to variations short term (5 year or less) variations in the wind stress.

For τ = 5 yrs (black curve in **Figure 6c**) the response in 2000 is ~85% of the equilibrium response and there are only very small changes after ~2010. In contrast, for τ = 50 yrs (blue curve in **Figure 6c**) there is a significant delay in the response: The response in 2000 is only ~25% of the equilibrium response, and by 2030 it is still on ~60% (i.e. the field is still decreasing 30 years after wind stress stopped increasing). In fact, it will not be until 2100 that response is 90% of equilibrium response.

The calculations in **Figure 6c** suggest that the BSF will have essentially reached its full response to the pre-2000 trends in wind stress by ~2010 and will not change (due to wind stress changes) over the next few decades. However, the mid-depth age, T and S within mode / intermediate waters will still be responding in the early 2000s and will continue to change for 3 or more decades even without a systematic change in the wind stress over this period, i.e. the impact of the wind stress trends at the end of the 20th century on mid-depth ocean properties could persist until the middle or even end of this century.

This smoothed, lagged response has important consequences for interpreting (inferring the cause of) observed changes in ocean properties. First, observed changes in subsurface fields should not be linked with simultaneous changes in wind stress but rather with a time-integrated (weighted) change in the wind stress. Second, it is possible there could a substantial decrease in the age (or increase in T and S) over a period with no trends in wind stress or BSF, which could be mistakenly interpreted as indicating trends in age, T and S are unrelated to wind stress of BSF changes.

Equation (2) provides insight into how to compare subsurface ocean changes with changes in the wind stress (i.e., to assess whether ocean changes are consistent with the wind stress changes). Differentiation of equation (2) yields

$$\frac{d\Phi}{dt}(t) = \int_0^t G(t-t')\frac{dF}{dt'}(t')dt' \,, \qquad (3)$$

where *G=dR/dt* (note, *G* differs from the passive tracer transit time distribution). For *R(t)* of the form (1) we have $G(t) = (R_0/\tau)e^{-t/\tau}$. Equation (3) implies a low-pass filter for changes in Φ compared to changes in *F*. A change (trend) in ocean property Φ (i.e., BSF, Γ, T, S) should then be compared with the time integral of the change (trend) in wind stress (F in equation 3) using weighting function G. For fields with a short response time τ (i.e. BSF) the integral (3) makes only a small difference and dΦ/dt~dF/dt, but for τ ~ 20-100 yrs there is a large difference in temporal variation of Φ and F (as shown in Fig. 4). In the latter case, the interior fields will be insensitive to interannual and 3-5 year variations (such as ENSO) in the wind stress (because of the decadal smoothing). In addition, any respond to wind stress changes will be delayed by decades.

6. Conclusions

Analysis of an idealized wind-stress perturbation experiment indicates that the response of the southern subtropical oceans to an increase in the surface winds occurs over multiple time scales, and varies among ocean properties. There is a relatively rapid (5-10 year) intensification of the subtropical gyres and deepening / shoaling of isopycnals in response to an increase in the surface winds. However, the decrease in age and increase in temperature and salinity in mode waters is generally much slower, with response time increasing from order 5 years near the surface to over 100 years at depths of 500-1000 m. The changes in sub-surface age, T and S at fixed depth occur because of changes in isopycnal depth (heaving), along-isopycnal transport, and (for T and S) changes in mixed layer properties which get transported into the interior. These processes occur on different time scales, resulting in a multi-time scale response for age, T and S. The time scale for along-isopycnal transport is much longer than for heave or mixed layer properties, and generally dominates the response time for age, T and S at fixed depth.

A slower response for subsurface tracer properties than the gyre circulation is not a surprise, but it is notable that the response time for the ideal age is much less than the ideal age itself. It might be expected that the response time is similar to the ideal age, as the ideal age is the mean time for transport from the surface to interior location. However, this is not the case for the age response in mode and intermediate waters to an increase in the wind stress. Analysis of the increase of ideal age and its response suggests the age response time is determined primarily by the advection of young waters to a given location, whereas the ideal age is much more strongly influenced by mixing with older (recirculated) waters to the location. Further research is required to determine if this is the case.

We have focused here on changes within the subtropical oceans within the first 100 years (the length of the simulation), but there are also changes outside this region. This includes the deep waters forming around Antarctica as well as the rest of the oceans. As mentioned in Section 4, there is a slow deepening of isopycnals north of 30^{o}S, consistent with a centennial timescale response of the global pycnocline and meridional overturning circulation (Jones et al. 2011; Allison et al. 2011).

The range of time scales for the response of different properties within the subtropical oceans to changes in the wind stress has consequences for the interpretation of observations. First, observed changes in subsurface fields should not be linked with simultaneous changes in wind stress but rather with a time-integrated (weighted) change in the wind stress (e.g. equation 3). For example, changes over a decade in the ideal age in mode waters should not be compared just with the wind stress changes over this period, but with changes over longer, multi-decadal period. Further, as the time scale of this weighting varies between fields and locations if there is a change in wind stress trends this may be observed in fast responding aspects of the oceans (e.g. horizontal circulation or density structure) but not in other properties (e.g., age, T and S in mode waters). This could mistakenly be taken to indicate that the changes in different properties are not driven by the same process.

The multi-decadal time scales for the subsurface response to changes in the wind stress also has consequence for current and projections of further changes. First, the subsurface fields will not be sensitive to less than decadal variations (e.g. ENSO) in the wnd stress. Further, there will generally be a large (decades) lag between projected changes in wind stress and

changes in subsurface fields. For example, wind-driven trends in age, T, and S in interior mode/intermediate waters may continue for several decades even if there is pause in the intensification and poleward shift of the summer wind stress (Banerjee et al. 2020, Barnes et al. 2014). This complicates attribution of observed changes in southern ocean mode waters to different natural and anthropogenic processes.

We plan to use these ideas in a comparison of repeat measurements of CFCs and SF_6 and changes in westerly winds over the southern oceans. Previous studies have analyzed measurements of these tracers made in the early 1990s and mid 2000s, and shown a decrease in ages within sub-Antarctic mode (e.g., Waugh et al 2013, Tanhua et al. 2013, Ting and Holzer 2015, Fine et al. 2017). Additional measurements have been made along the same ocean sections in the last few years, which allows the opportunity to also estimate the change in age from mid 2000s to mid-late 2010s. The evolution of age at different depths can then be compared with time-integrated changes in winds to test whether the changes in age can be attributed to the wind changes.

Acknowledgments

We thank P. Gent, G. Danabasoglu, F. Bryan and M. Long for discussions and advice regarding the CCSM4 simulations; and A Hogg for helpful discussions and comments on the manuscript. The CCSM4 data presented is archived on the Johns Hopkins University Data Archive at https://archive.data.jhu.du/dataverse/.

References

Allison, L.C., Johnson, H.L. & Marshall, D.P. (2011), Spin-up and adjustment of the Antarctic Circumpolar Current and global pycnocline. *Journal of marine research*, *69*(2-3), pp.167-189.

Anderson, D. L. T., & Killworth, P. D. (1977), Spin-up of a stratified ocean, with topography. *Deep-Sea Res*., 24, 709–732.

Anderson, D.L., Bryan, K., Gill, A.E. & Pacanowski, R.C. (1979), The transient response of the North Atlantic: Some model studies. *Journal of Geophysical Research: Oceans*, *84*(C8), 4795-4815.

Banerjee A, JC Fyfe, L. M Polvani, & D.W. Waugh (2020), A pause in Southern Hemisphere circulation trends due to the Montreal Protocol, *Nature* **to appear**.

Barnes, E.A., Barnes, N.W. & Polvani, L.M. (2014), Delayed Southern Hemisphere climate change induced by stratospheric ozone recovery, as projected by the CMIP5 models. *Journal of Climate*, *27*, 852-867.

Bindoff, N. L., & T. J. Mcdougall, 1994: Diagnosing climate change and ocean ventilation using hydrographic data. *J. Phys. Oceanogr.,* 24, 1137–1152.

Boning, C. W., Dispert, A., Visbeck, M., Rintoul, S. R. & Schwarzkopf, F. U. 2008: The response of the Antarctic Circumpolar Current to recent climate change. *Nature Geosci*. 1, 864-869.

Cai, W., Cowan, T., Godfrey, S., & Wijffels, S. 2010: Simulations of processes associated with the fast warming rate of the southern midlatitude ocean. *J. Climate*, 23, 197-206.

Deser, C., Alexander, M.A. & Timlin, M.S., 1999: Evidence for a wind-driven intensification of the Kuroshio Current Extension from the 1970s to the 1980s. *Journal of Climate, 12*, 1697-1706.

Downes, S. M., C. Langlais, J. P. Brook, & P. Spence, 2017: Regional impacts of the westerly winds on Southern Ocean Mode and Intermediate Water subduction. *J. Phys. Oceanogr*., 47, 2521–2530.

England, M.H., 1995: The age of water and ventilation timescales in a global ocean model. *J Phys. Oceanogr*., *25*, 2756-2777.

Farneti, R, T. L. Delworth, A. J. Rosati, S. M. Griffies, & F. Zeng, 2010: The role of mesoscale eddies in the rectification of the Southern Ocean response to climate change. *J. Phys. Oceanogr.,* 40, 1539–1557.

Ferreira, D., J. Marshall, C. M. Bitz, S. Solomon, & R. A. Plumb, 2015: Antarctic Ocean and sea ice response to ozone de- pletion: A two-time-scale problem. *J. Climate*, 28, 1206–1226.

Fine, R.A., Peacock, S., Maltrud, M.E. and Bryan, F.O., 2017. A new look at ocean ventilation time scales and their uncertainties. *Journal of Geophysical Research: Oceans*, *122*(5), pp.3771-3798.

Gao, L., Rintoul, S.R. & Yu, W., 2018. Recent wind-driven change in Subantarctic Mode Water and its impact on ocean heat storage. *Nature Climate Change*, *8*, 58.

Gent, P.R., & G. Danabasoglu 2011 Response to Increasing Southern Hemisphere Winds in CCSM4, J Climate, 4992-4998.

Gent, P.R., Danabasoglu, G., Donner, L.J., Holland, M.M., Hunke, E.C., Jayne, S.R., Lawrence, D.M., Neale, R.B., Rasch, P.J., Vertenstein, M. and Worley, P.H., 2011. The community climate system model version 4. *Journal of Climate*, *24*(19), pp.4973-4991.

Hasselmann, K., Sausen, R., Maier-Reimer, E. & Voss, R., 1993: On the cold start problem in transient simulations with coupled atmosphere-ocean models. *Climate Dynamics, 9*, 53-61.

Hall, T.M., & T.W.N. Haine 2002: On Ocean Transport Diagnostics: The Idealized Age Tracer and the Age Spectrum, J. Phys. Ocean., 1987-2001.

Hogg, A. M., P. Spence, O. A. Saenko, & S. M. Downes, 2017: The energetics of Southern Ocean upwelling. J. Phys. Oceanogr., 47, 135–153.

Jones, D. C., T. Ito, and N. S. Lovenduski (2011), The transient response of the Southern Ocean pycnocline to changing atmospheric winds, Geophys. Res. Lett., 38, L15604, doi:10.1029/2011GL048145.

Le Quere, C., Rödenbeck, C., Buitenhuis, E.T., Conway, T.J., Langenfelds, R., Gomez, A., Labuschagne, C.Ramonet, M., Nakazawa, T., Metzl, N. & Gillett, N. 2007 Saturation of the Southern Ocean CO2 sink due to recent climate change. Science, 316, 1735-1738

Marshall, J., Armour, K.C., Scott, J.R., Kostov, Y., Hausmann, U., Ferreira, D., Shepherd, T.G. & Bitz, C.M., 2014. The ocean's role in polar climate change: asymmetric Arctic and Antarctic responses to greenhouse gas and ozone forcing. *Phil. Trans. R. Soc. A*, *372*(2019).

Roemmich, D., J Gilson, R. Davis, P. Sutton, S. Wijffels, & S. Riser, Decadal Spinup of the South Pacific Subtropical Gyre, J. Phys. Ocean., 37, 162-, 2007.

Roemmich, D., Gilson, J., Sutton, P. & Zilberman, N., 2016. Multidecadal change of the South Pacific gyre circulation. *Journal of Physical Oceanography*, *46*(6), pp.1871-1883.

Russell, J.L., Dixon, K.W., Gnanadesikan, A., Stouffer, R.J. and Toggweiler, J.R., 2006. The Southern Hemisphere westerlies in a warming world: Propping open the door to the deep ocean. *Journal of Climate*, *19*(24), pp.6382-6390.

Sen Gupta, A., & M.H. England, 2006: Coupled Ocean–Atmosphere–Ice Response to Variations in the Southern Annular Mode, *J Climate*, 19.

Sijp, W. P., & M. H. England, 2008: The effect of a northward shift in the southern hemisphere westerlies on the global ocean. *Prog. Oceanogr*., 79, 1–19

Spence, P., S. M. Griffies, M. H. England, A. M. Hogg, O. A. Saenko, & N. C. Jourdain, 2014: Rapid subsurface warming and circulation changes of Antarctic coastal waters by pole- ward shifting winds. *Geophys. Res. Lett*., 41, 4601–4610

Swart, N.C. & J.C. Fyfe, 2012: Observed and simulated changes in the Southern Hemisphere surface westerly wind-stress, *Geophys. Res. Lett.,* 39, L16711, doi:10.1029/2012GL052810

Tanhua, T., D. W. Waugh, & J. L. Bullister, 2013: Estimating changes in ocean ventilation from early 1990s CFC-12 and late 2000s SF_6 measurements, *Geophys. Res. Lett.,* 40, 927–932, doi:10.1002/grl.50251.

Thomas, M.D., De Boer, A.M., Johnson, H.L. & Stevens, D.P., 2014: Spatial and temporal scales of Sverdrup balance. *Journal of Physical Oceanography*, *44*, 2644-2660.

Thompson DWJ, Solomon S, Kushner PJ, England MH, Grise KM, Karoly DJ. 2011: Signatures of the Antarctic ozone hole in Southern Hemisphere surface climate change. *Nat. Geosci.* 4, 471–479

Ting, Y.H. & Holzer, M., 2017: Decadal changes in Southern Ocean ventilation inferred from deconvolutions of repeat hydrographies. *Geophysical Research Letters*.

Waugh, D. W., F. Primeau, T. DeVries, & M. Holzer 2013 Recent changes in the ventilation of the southern oceans, *Science*, 339, 568.

Waugh, D.W. (2014). Changes in the ventilation of the southern oceans, *Philosophical Transactions A.,* 373, 0130269.

Waugh, D.W., A. Mc C. Hogg, P Spence, M. H. England, T. W.N. Haine, 2019: Response of Southern Ocean ventilation to changes in mid-latitude westerly winds, *J Climate*, 32, 5345-5361.

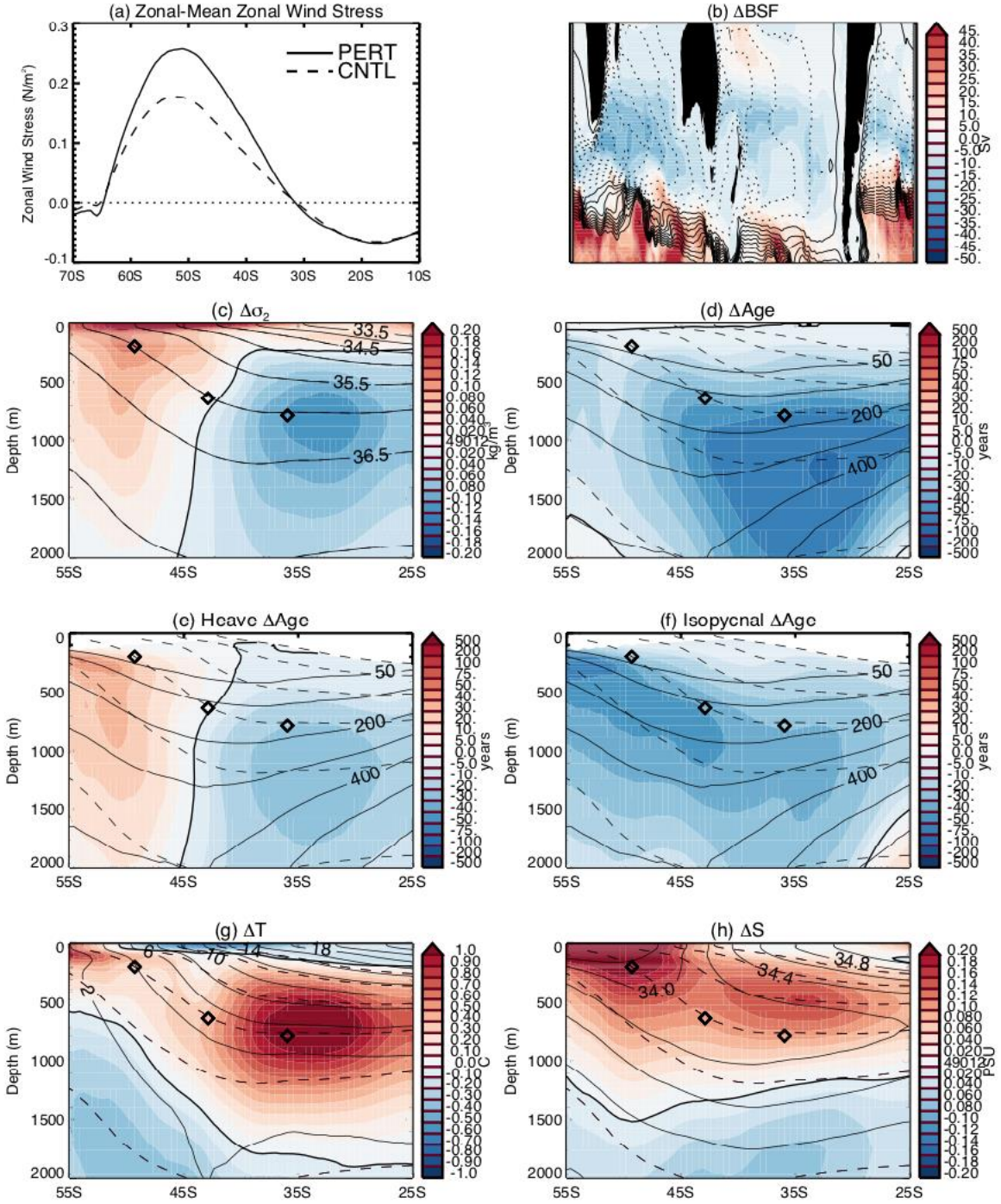

Figure 1: (a) Latitudinal variations of the time-mean zonal-mean zonal wind stress for the Control and Perturbation simulations. (b) Map of barotropic stream function, and latitude-height plots of zonal-mean (c) σ_2, (d) total, (e) heave, (f) isopycnal change in age, (g) T, and (h) S. Shading shows response (Perturbation-Control) at year 100 (with the heavy black contour showing zero response), solid contours show for Control simulations at year 100, and dashed contours show isopycnal surfaces σ_2 = 33.5, 34.0, … 37.0 kg/m^3.

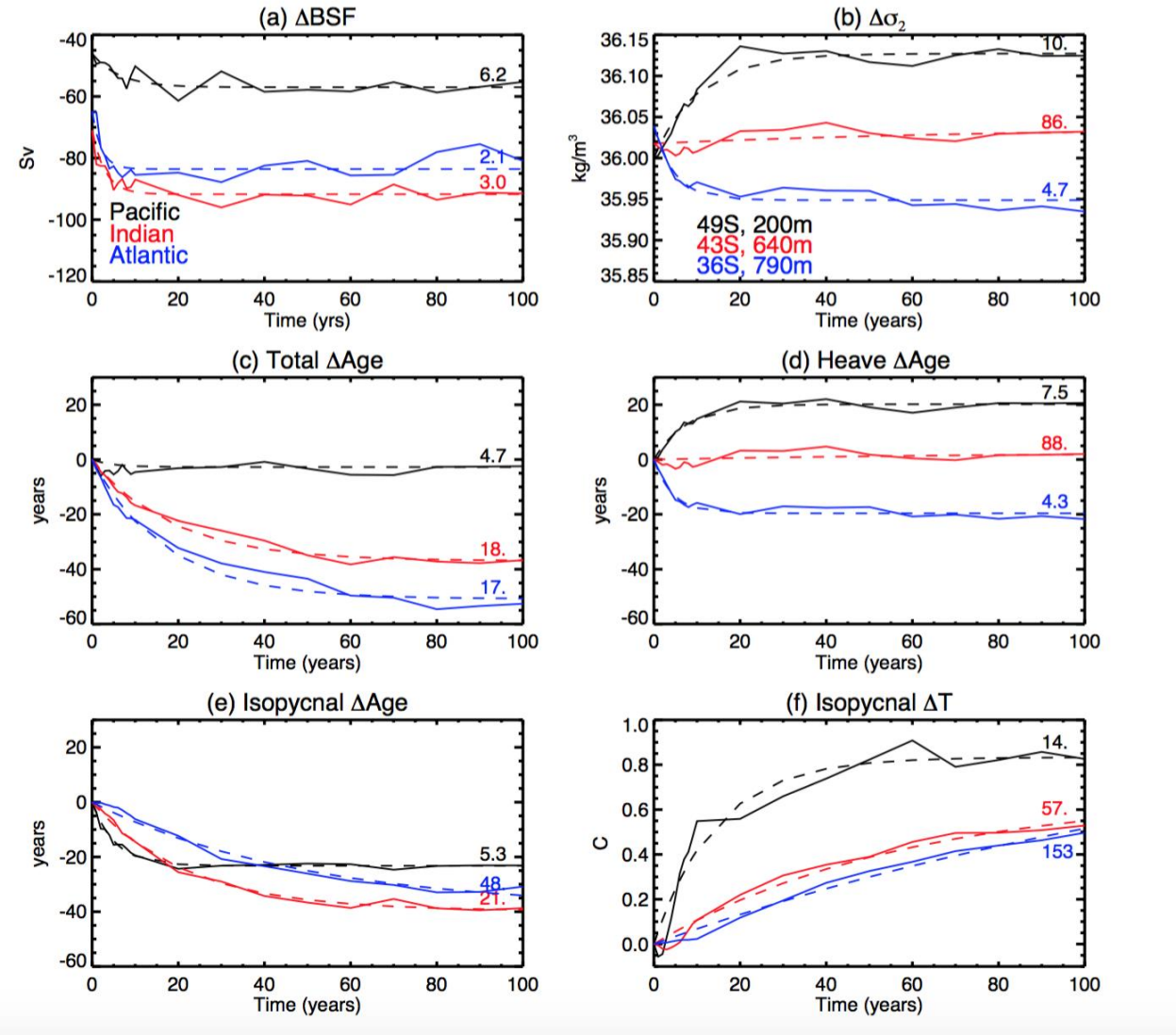

Figure 2: Time series of change in (a) minimum BSF in Pacific, Indian, and Atlantic oceans, (b) potential density, (c) age, (d) heave age, (e) isopycnal age, and (f) isopycnal T. (b)-(f) show zonal-mean values 49°S, 200m, 43°S, 640m, and 36°S, 790m, which all lie on the σ_2=36 kg/m^3 surface (see diamonds in Fig 1). Dashed curves show fit using equation (1), and corresponding response time τ is listed above curves.

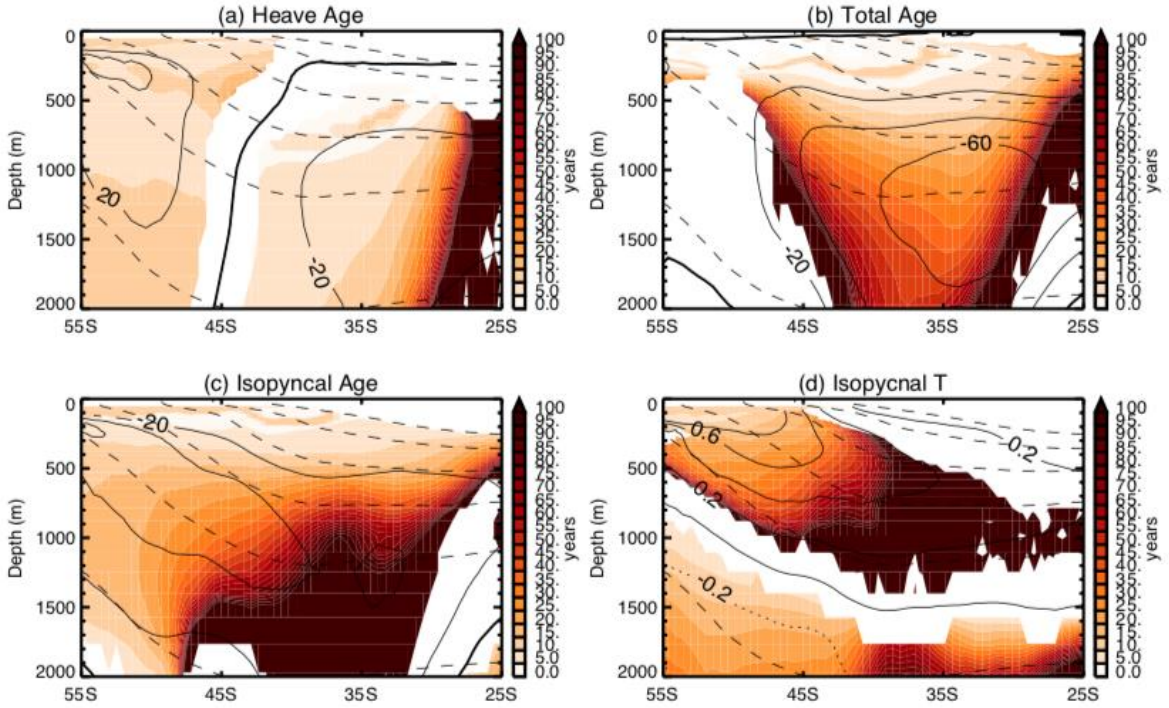

Figure 3: Latitude-height plots of response time τ for (a) potential density and heave change in age, (b) total change in age, (c) isopycnal change in age, and (d) isopycnal change in T and S. Solid contours show response (Perturbation-Control) at year 100 and dashed contours show isopycnal surfaces σ_2 = 33.5, 34.0, … 37.0 kg/m^3.

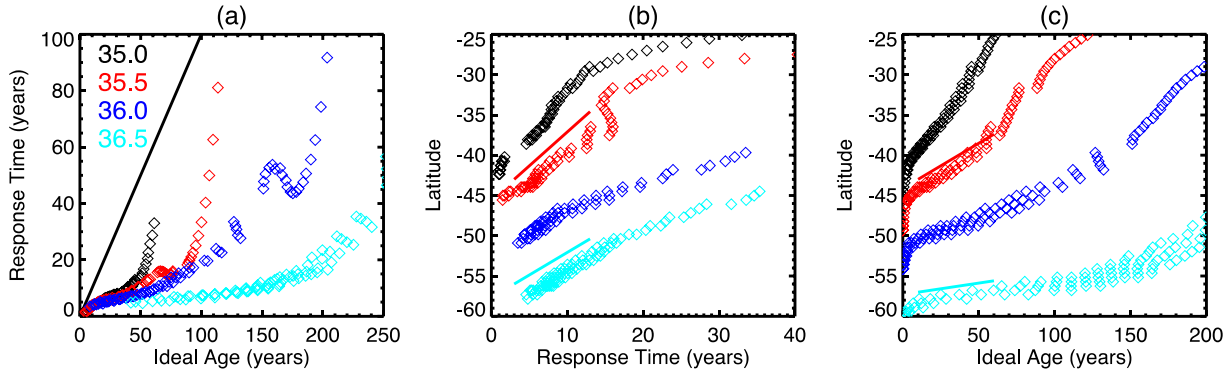

Figure 4: Variation of (a) response time and (b) ideal age with latitude, for 35, 35.5, 36.0, and 36.5 kg/m^3 isopycnal surfaces. Solid lines correspond to linear latitude-time relationships with slopes of 0.2 cm/s (blue) and 0.3 cm/s (red) in panel (a), and of 0.01 cm/s (blue) and 0.04 cm/s (red) in panel (b). (c) Variation of response time of ideal age with ideal age for same isopycnal surfaces as in (a) and (b).

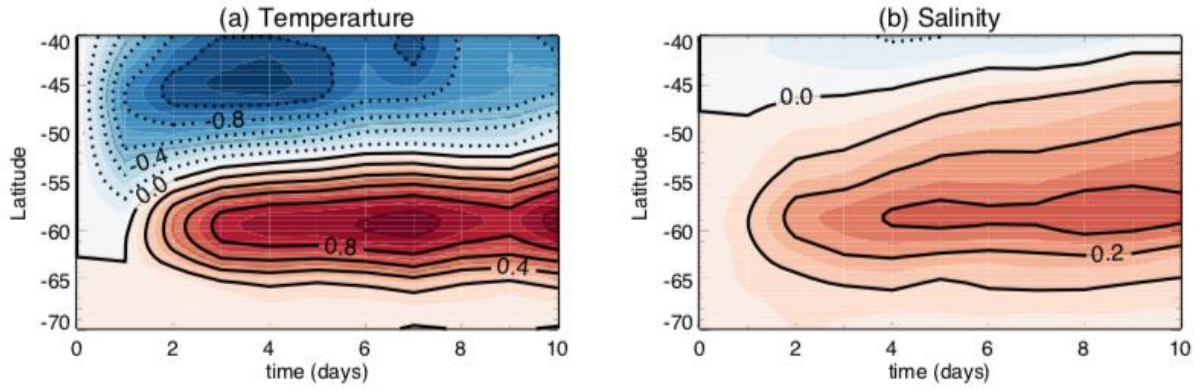

Figure 5: Temporal evolution of anomalies in zonal-mean (a) temperature and (b) salinity at 5m. Anomalies are deviations from initial values.

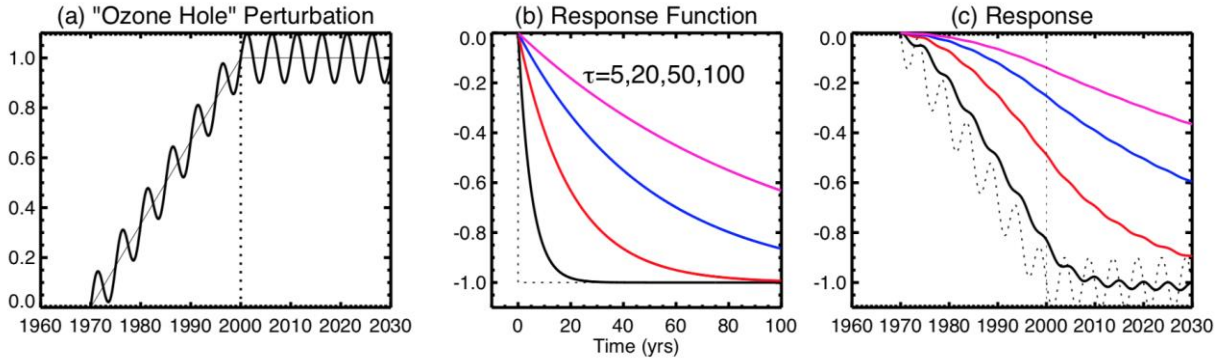

Figure 6: (a) wind stress perturbation mimicking changes due to ozone depletion and stabilization, (b) response functions (R) given by equation 1 with τ = 5, 20, 50, and 100 yrs, and (c) response to perturbation (a) for R(t) shown in (b). All fields normalized.